Available online at BCREC website: https://bcrec.id

Bulletin of Chemical Reaction Engineering & Catalysis, 17 (3) 2022, 542-553

Research Article

Investigating the Interaction between Methanol and the Heulandite-type Zeolite using First Principle Molecular Dynamic

Fiska Dewi Wulandhani, Fajar Inggit Pambudi*

Department of Chemistry, Universitas Gadjah Mada, Sekip Utara BLS 21 Yogyakarta, 55281, Indonesia.

Received: 14th July 2022; Revised: 26th August 2022; Accepted: 26th August 2022
Available online: 30th August 2022; Published regularly: September 2022

Abstract

The interaction between methanol and the Heulandite-type zeolite has been unveiled to give an atomic scale detail regarding the catalytic activity of this zeolite for methanol conversion. The study was carried out by first principle molecular dynamics to get an insight into the structure and electronic behaviour of methanol inside the zeolite structure at different temperatures. The behaviour of methanol was studied when the location of the proton of Brönsted acid sites was varied to give both possible direct and less interaction with methanol. The results show that methanol interacts with the proton from zeolite to give a cationic species of $[CH_3OH_2]^+$ both in 300 and 573 K conditions. However, when the proton is located at different location far from possible interaction with methanol, the formation of a cationic species is hindered. This study provides an insight into the design of Heulandite type zeolite to give a catalytic activity toward methanol transformation.

Keywords: Zeolite; heulandite; methanol; ab initio molecular dynamic; structure

How to Cite: F.D. Wulandhani, F.I. Pambudi (2022). Investigating the Interaction between Methanol and the Heulandite-type Zeolite using First Principle Molecular Dynamic. *Bulletin of Chemical Reaction Engineering & Catalysis*, 17(3), 542-553 (doi: 10.9767/bcrec.17.3.15169.542-553)

Permalink/DOI: https://doi.org/10.9767/bcrec.17.3.15169.542-553

1. Introduction

Zeolite is a class of nanoporous materials which have periodic arrangement of aluminosilicate to give various archetypes of porosity [1,2]. Currently, there are approximately 255 different topologies which have been reported in the International Zeolite Database [3]. Many of those topologies are reported as synthetic zeolites, but there are also many zeolite topologies which are formed naturally through possible geological activities. Several examples of naturally occurring zeolite are mordenite (MOR), heulandite (HEU), stilbite (STI), chabazite (CHA), offretite (OFF) *etc.* [3,4]. Many of natural zeolites have been successfully synthesised as their counterpart to further modify their structural behaviour or functionality towards many applications [5–7].

Computational studies on the interaction of zeolite and guest molecule have been reported in many literatures to understand the potential application of zeolite in many areas. Several examples are given such as the confinement of water cluster in zeolite pore to give an insight into the fate of water inside the bulk zeolite [8–10]. Besides water cluster, the interaction between alcohols and zeolite have been studied computationally highlighting the significance important of atomic level interaction [11,12]. Another host-guest study is the computational study on the adsorption of aromatic compounds, such as ben-

* Corresponding Author.
Email: fajar.inggit@ugm.ac.id (F.I. Pambudi)

zene, toluene and naphthalene [13]. However, the used of zeolite as heterogenous catalyst is one of the most important aspects in zeolite application. The computational studies on the catalytic activity of zeolite towards methanol transformation have been reported highlighting the complex reaction that might occur due to simple interaction between methanol and zeolite [14,15]. Most of the studies are utilizing first principle calculation, such as density functional theory as well as modelling through classical molecular dynamics.

Owing to the zeolites structure diversity, they have been used in industrial process particularly in catalysis technology. Currently, transforming methanol into more valuable chemical precursors becomes an important process in industry. However, catalysts are usually required to give an efficiency and selectivity towards the product of methanol transformation [16,17]. Many zeolite topologies have been studied in term of their catalytic performance toward the conversion of methanol to other valuable chemicals [18–21]. However, modification of the zeolite surface is also possible to increase the efficiency and selectivity of the product by incorporating various metal, such as Cu, Ni, Pd etc. For example LTA type zeolite has been investigated towards their catalytic activity for methanol oxidation reaction by introducing metal ions, such as Cu and Ni [22]. Another study shows that the confinement effect of the zeolite cavities might also affect the methanol conversion to olefin [23].

Heulandite type zeolite as a part of natural zeolite has been reported in term of its synthetic strategies for modifying the surface functionality and stability [24,25]. Heulandite is usually found to have a low Si/Al ratio (<6) which sometimes contains metal ions impurities. In recent study, synthetic Heulandite type zeolite was reported to have higher Si/Al ratio up to 9.8 [25]. This opens new possibilities to use this zeolite in many applications particularly catalysis. Heulandite contains three different pore environment which can be used as a space for guest molecules during catalytic activity. The largest pore in Heulandite structure is a 10-member ring (10MR) with the size of approximately 11 Å which is large enough to host small molecules, such as methanol. Two other pores of 8MR channels have diameter of approximately 7 Å. Heulandite and its isostructural type which is clinoptilolite have been reported for several applications such as adsorption of hydrocarbon [26,27] and water [28,29], cation exchange [30] and catalysis [31]. However, reports about the interaction between methanol and Heulandite type zeolite is still scarce.

In this study, the structural behaviour of methanol inside the cavity of Heulandite type zeolite is reported. Methanol was placed inside the largest pore (10MR ring) to identify its interaction with the surface of Heulandite. The Heulandite structure was modified to accommodate Al atom distribution which is following the Lowenstein rule. However, the acid sites were situated at two different positions where methanol in the largest pore is able to interact with the proton and the second configuration is that the proton is inaccessible to methanol within the 10MR ring. To unveil the behaviour of methanol inside the Heulandite structure, first principle molecular dynamics were conducted at two different temperatures of 300K and 573K.

2. Materials and Methods

2.1 Computational Methods

The crystal structure was taken from the International Zeolite Database (IZA) with the code HEU. All density functional theory (DFT) calculations were performed within CP2K module [32]. DFT calculation was performed to optimize the initial structure of all silica Heulandite structure and Al-substituted heulandite with Si/Al ratio of 11. The position of Al was adjusted to follow the Lowenstein rule and positioned at the crystallographic sites of T2 and T3 sites. The selection of this sites follows our previous report where the Al atoms will be relatively stable if they are positioned in T2 and T3 sites [13]. Geometry optimization was performed using the generalized gradient approximation of Perdew-Burke-Ernzerhof (PBE) functional with DZVP basis set for every atom. This selection of basis set was thoroughly studied in previous study to obtain optimized structures which conform to the reported literature [13]. Goedecker-Teter-Hutter (GTH) pseudopotential was used to treat the core electrons. An energy cut-off of 450 Ry was used throughout the calculations. The convergence criteria for the self-consistent field was set to be 1×10^{-5} Hartree with the maximum force of 0.00045 Hartree/Bohr. Single point energy was used to examine the energy and electronic properties by employing auxiliary density matrix method (ADMM) with the hybrid DFT method of HSE06 with 25% of the short-range Hartree-Fock exchange (HFX) and Grimme D3 van der Waals correction. The total charge of the zeo-

lite structure and methanol was calculated following the Mulliken partition method for all atoms in the unit cell.

Ab initio molecular dynamics (AIMD) were conducted on four configurations. The first structure is the Heulandite zeolite with the Si/Al ratio of 11. The second and third configurations are the Heulandite structure in the presence of a methanol molecule at two different temperatures of 300 and 573 K. Methanol with the molecular size of 2.372 Å was located inside the 10MR ring. In this case, one of the protons of Brönsted acid is located on the surface of 10MR which is in direct contact with methanol. The fourth configuration is the Heulandite zeolite with methanol, but the location of the proton was adjusted to be inaccessible to methanol in the 10MR cavity.

The structural dynamics of Heulandite and its interaction with methanol were examined using AIMD with the basis set of DZVP for every atom. The PBE functional was used with the addition of the D3 dispersion correction scheme by Grimme (DFT-D3). An energy convergence for the self-consistent field (SCF) calculation was set to 1×10^{-5} Hartree and calculated using the limited-memory of Broyden-Fletcher-Goldfarb-Shanno algorithm. An energy cutoff of 450 Ry was used in all AIMD simulations. The calculations were performed under NVT at temperatures of 300 and 573 K. The timestep of the integration of motion was set to 0.5 fs. A canonical sampling through velocity rescalling (CSVR) thermostat was used to control the temperature with a time constant of 50 fs. The changes in atomic coordinates were stored in trajectory files. An equilibrium phase was set to 2.5 ps followed by the production phase of 7.5 ps. All data reported here are based on the production phase.

3. Results and Discussion

3.1 Structural Dynamics of the Heulandite-type Zeolite

The stability of zeolite structure can be estimated according to the number of Al components in the structure. It is known that the lower ratio of Si to Al lead to the less thermal stability of the structure [33]. To unveil the characteristic of all silica Heulandite and the presence of Al within the structure, DFT calculation was performed with the structures given in Figure 1. The optimized structure of all silica Heulandite has been confirmed to have unit cell parameters of a = 17.5823 Å, b = 17.7341 Å and c = 7.4295 Å. These unit cell dimensions are in accordance with the experimental data obtain from the X-ray diffraction experiment and from the IZA database with a = 17.520 Å, b = 17.640 Å, and c = 7.400 Å. However, the unit cell dimensions reported in the literatures can

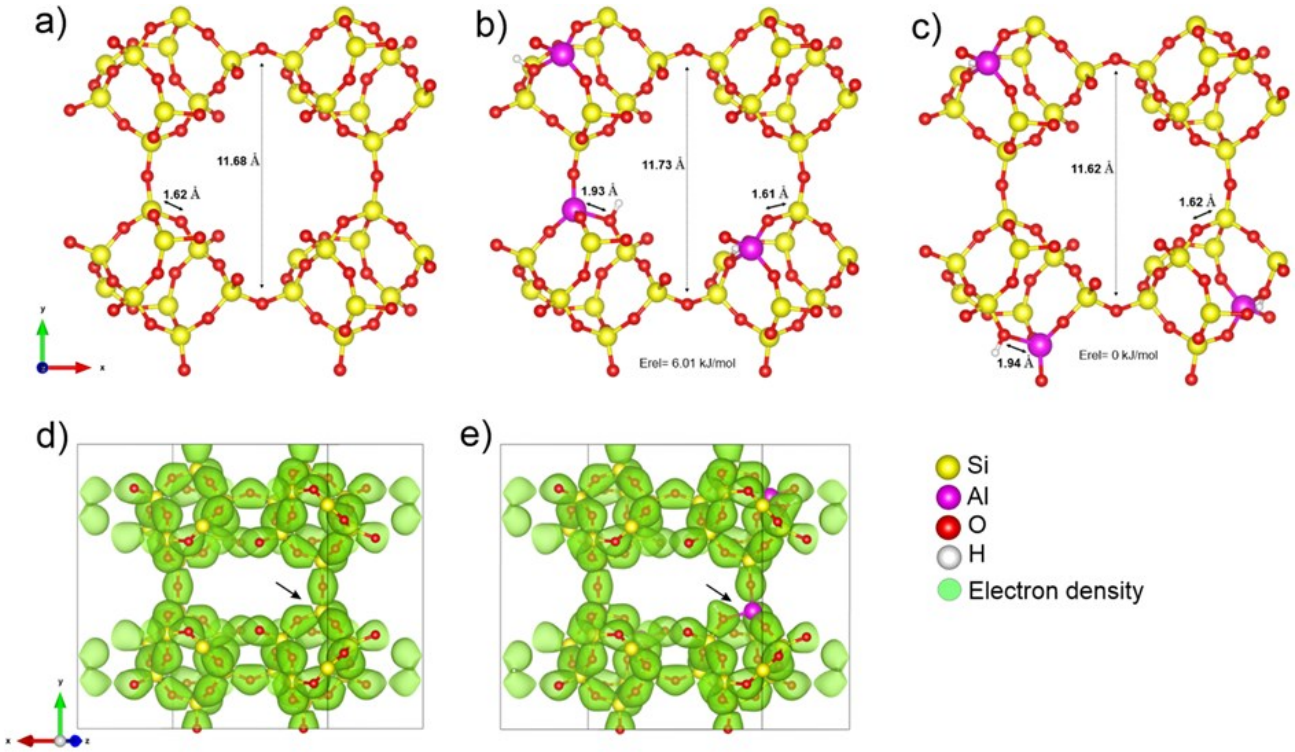

Figure 1. The structure of all silica Heulandite (a), Heulandite with Si/Al of 11 with various location of Al (b-c). The electron density of all silica Heulandite (d) and Al-substituted Heulandite (e) is also given.

vary depending on the experimental set up and the condition of the samples such as the presence of cations within the heulandite structure or activated samples [34,35]. In term of the bond distance especially Si–O, it has a length of approximately 1.62 Å. This bond distance is similar to the reported value of 1.6 Å [36,37].

The presence of Al within the structure is clearly disturb the structural characteristic of all silica Heulandite. This can be observed from the bond distance of Al–O which has bond length of 1.70 Å. This is relatively longer than the bond distance in Si–O. However, Al connected to O(H) has greater bond length of 1.93 Å as shown in Figure 1(b) and (c). The significance of longer bond in Al–O may correlate with their stability as lower Si/Al ratio tends to give a lower structural stability. The correlation between bond length and the ratio of Si/Al has an impact to the stability of zeolite. As the number of Al in the zeolite structure increases, it has more Al–O bond which is longer in bond distance than Si–O bond. A longer bond distance due to Al–O can be related to the ease of bond breaking compared to the shorter bond in Si–O. Therefore, a high Si/Al ratio is preferably to maintain the structural stability due to small number of Al. The coordination nature between Si and O as well as Al and O can be observed from the electron density given in Figure 1(d) and (e). In all silica heulandite (Figure 1(d)), the electron density around Si–O bond is relatively close in gap. However, when Si is replaced with Al, the electron density around Al–O has longer gap as illustrated with the black arrow in Figure 1(d) and (e). This implies that the coordination nature of Si–O is relatively stronger than Al–O. Therefore, designing zeolite material with relatively higher Si/Al ratio is benefit to the structural stability.

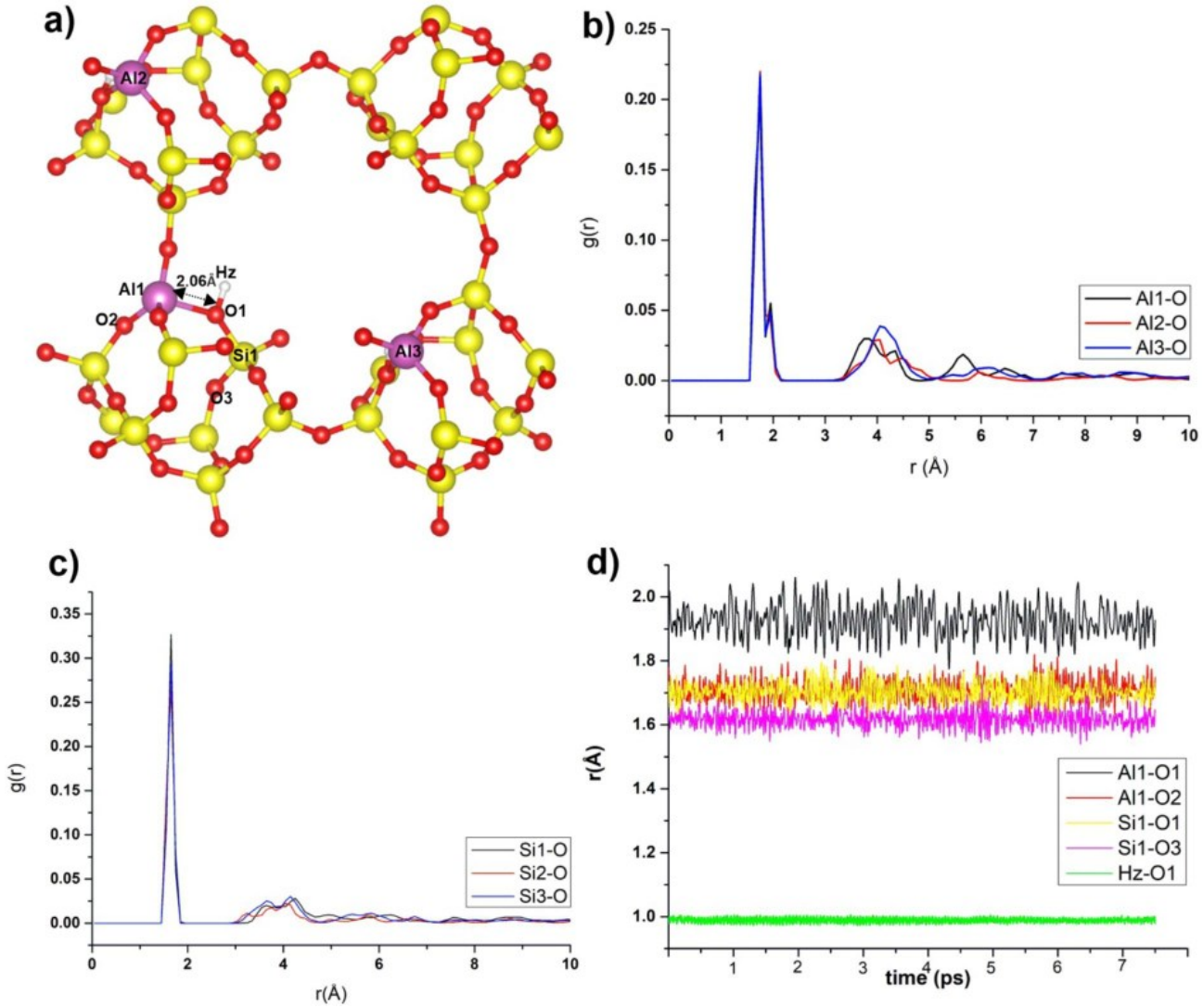

Figure 2. The structure of HEU type zeolite showing the location of Al atoms and bond distance with the longest Al1–O1 distance in AIMD simulation (a). RDFs of Al and Si to O atoms are shown in (b) and (c) while the evolution of several bond distance along the production phase of AIMD is given in (d).

The position of Al within the structure also affects the structural characteristics especially the size of the pore such as diagonal pore size as given in Figure 1(a)-(c). In all silica Heulandite, the size of the diagonal pore is approximately 11.68 Å which is expanding when Al is positioned in the 10MR ring to give a diagonal pore of 11.73 Å (see Figure 1(b)). However, when Al is positioned far from the 10MR (Figure 1(c)), the diagonal pore is at 11.62 Å. In term of the energy of the structure, this study provides two different positions of Al within the structure of Heulandite as shown in Figure 1(b) and (c). The first structure corresponds to the location of Al within the 10MR ring, while the second structure is Al with the location not on the surface of 10MR ring. The second structure is relatively more stable than the first structure with energy different of only approximately 6 kJ/mol. This energy range is still within the reported energy range [13]. In this study, the Al atom is located in T2 and T3 sites in accordance with the previous experimental and computation studies [37,38].

The structural behaviour of the Heulandite zeolite in the presence of Al (Si/Al ratio of 11) was also examined through AIMD. As seen in Figure 2(a), the bond length of Si−O is in average 1.60 Å similar to the reported value for other zeolite types, such as mordenite and chabazite [36,37]. This is confirmed by the radial distribution function (RDF) of Si to O given in Figure 2(c). However, when Si is connected to O atom which is bonded with hydrogen (O1), the Si−O1 distance increases slightly to 1.71 Å. In case for Al−O, there is an elongation of bond distance. The evolution of Al−O and Si−O distance was examined as seen in Figure 2(b) and (d) based on the type of oxygen atom connected to Al. An example is given for Al1 which is connected to O2 to give an average bond distance of 1.71 Å. However, Al1 connected to O1 with hydrogen in its neighbour has slightly longer bond distance of 1.93 Å in average with the longest bond distance during 7.5 ps of production phase is 2.06 Å as seen in Figure 2(a). Another type of important interaction is the distance between O1(zeolite) and hydrogen as the Brönsted acid sites. The hydrogen is stabilized in the zeolite pore located close to Al atoms particularly on the O atom with a distance of 0.98 Å (see Figure 2(d)). The spatial location of hydrogen will probably determine the interaction with guest molecules such as methanol.

3.2 Interaction of Methanol with HEU

In this study, a molecule of methanol was placed inside the 10MR ring in the Heulandite structure as given in Figure 3. The optimized structure from static DFT in Figure 3 indicates possible interaction between methanol and the surface of 10MR ring especially at the hydrogen from the zeolite as Brönsted acid site. The adsorption energy is calculated to be −147.2 kJ/mol indicating an exothermic process. Looking at the structural behavior, it shows that the hydrogen of zeolite (Hz) is located approximately 1.21 Å from the oxygen of zeolite. This distance is relatively longer than Hz to oxygen of zeolite (0.98 Å) without the presence of methanol (see Figures 1(b) and 2(d)). This indicates an interaction between hydrogen of zeolite (Hz) and oxygen of methanol (Om). Further examination is observed from the electron density around methanol as shown in Figure 3(b). There is an overlap of electron densities that

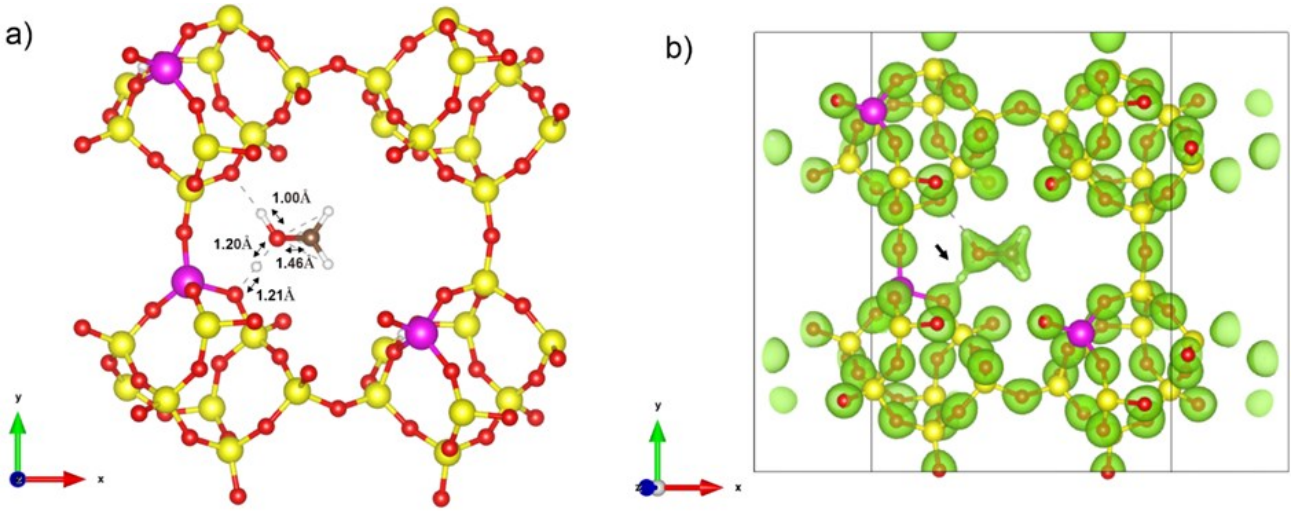

Figure 3. The optimized structure (a) and electron density (b) of Heulandite in the presence of methanol.

occur at oxygen of zeolite, Hz and methanol as highlighted with the black arrow.

To unveil the structural behaviour, AIMD is performed to reveal the interaction nature of methanol with Heulandite. The calculations were performed at 300 and 573 K. The temperature was chosen to compare the behaviour of methanol inside the Heulandite framework at approximately room temperature (300 K) and elevated temperature (573 K). In addition, the temperature at 573 K has been reported experimentally to be the induction period where the transformation of methanol has been occurred to give the products such as olefins and light hydrocarbons [16]. However, a higher temperature has also been reported for methanol transformation.

The first observation is for the Al–O and Si–O bond distance at different temperature (see Figure 4(a)). At 300 K, the Al–O distance is approximately 1.85 Å and it increases slightly to 1.87 Å at 573 K. The same observation is also given for Si–O bond with the length of 1.66 Å at 300K and 1.67 Å at 573 K. This observation confirms that zeolite is very stable at high temperature (in this case 573 K) without

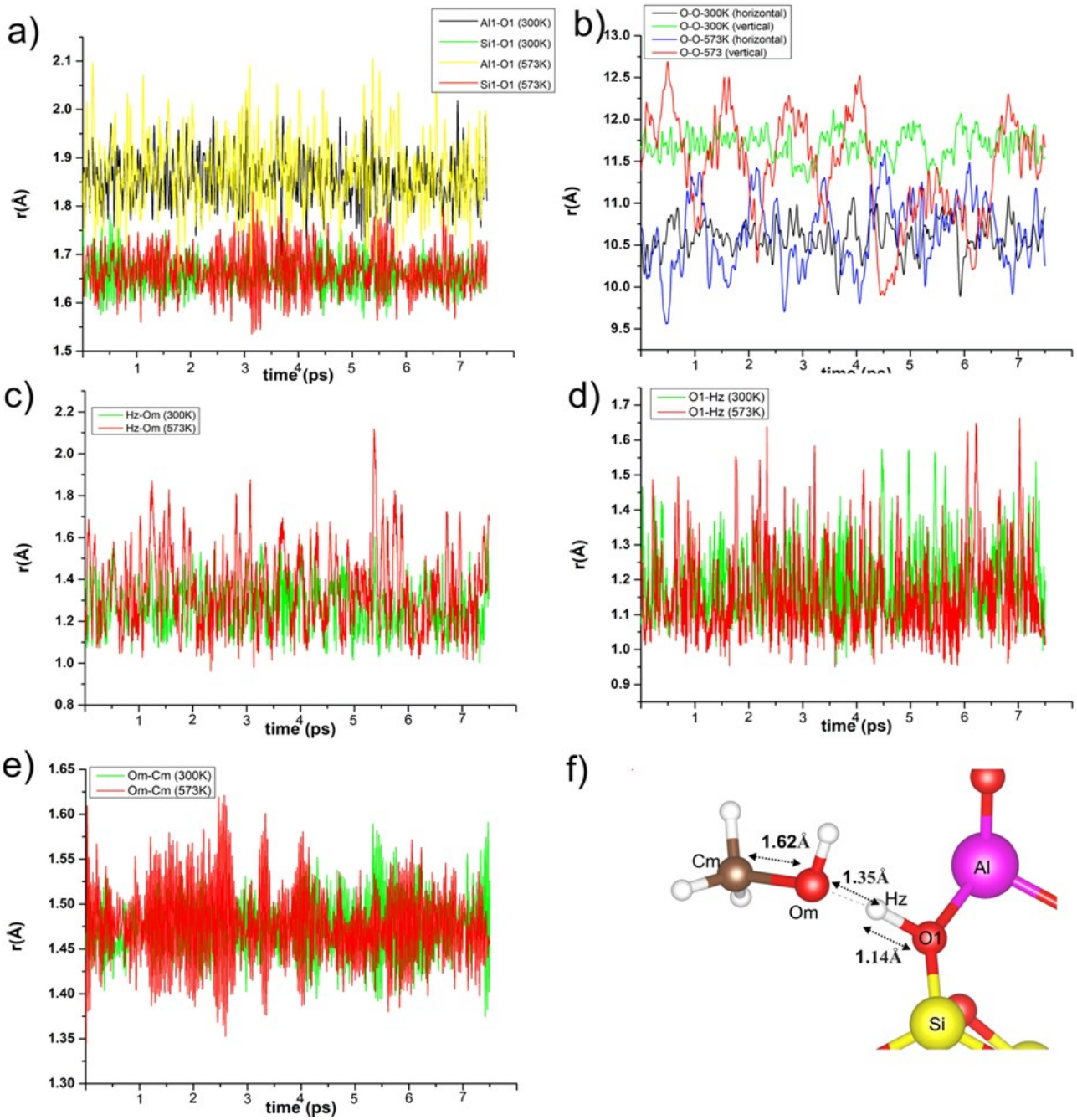

Figure 4. The bond distance of several structural composition in Heulandite type zeolite in the presence of methanol (a-e) and interaction between methanol and the proton of Brönsted acid sites (f).

significant changing in its structural integrity. However, the number of Al in the framework might influence the structural stability as the lower Si/Al ratio led to less stability than the one with higher Si/Al ratio. Difference in temperature also affects the size of the diagonal pore in Heulandite structure as shown in Figure 4(b). The size of the 10MR pore indicated by horizontal and vertical diagonal show an oscillating behaviour especially at 573 K. The vertical size of the 10MR pore is approximately 11.7 Å which is longer than the horizontal size at 10.5 Å measured from two oxygen atoms at the longest distance (see Figure 4(b)).

The structural behaviour of methanol inside zeolite structure is unveiled based on the hydrogen of zeolite (Hz) to oxygen of zeolite (O1) (Hz−O1) (Figure 4(d)), Hz to oxygen of methanol (Om) (Hz−Om) (Figure 4(c)), and Om to carbon of methanol (Cm) (Om−Cm) (Figure 4(e)). In the first case (Hz−O1), the absence of methanol in the zeolite structure gives bond length of Hz−O1 to be 0.98 Å which then increase in length due to the presence of methanol within the pore. At 300 K, the Hz−O1 bond length is at 1.00 Å at the lowest up to 1.62 Å at the highest in the presence of methanol. The same observation occurred at 573 K, where the Hz−O1 bond length increase to 2.12 Å at the longest distance as seen in Figure 4(d). The elongated bond occurs due to the interaction between hydrogen (Hz) as the Brönsted acid and the oxygen of methanol (Om) (Figure 4(c)) to give a methoxonium molecule $[CH_3OH_2]^+$. The presence of methoxonium ion has been investigated in previous study both experiment and computational studies (see Table 1). This ion is the initial precursor for further transforming methanol into various chemicals through many possible pathways, such as carboncation mechanism, carbene mechanism, free radical mechanism, *etc.* [16]. In our calculation, the methoxonium ion has been formed as the precursor of possible various chemicals such as olefins and light hydrocarbons. Previous studies have also confirmed that such ionic species might occur during the interaction of methanol and the Brönsted acid sites of zeolite such as in MFI and ZSM-5 [14,15]. Additional several studies are listed in Table 1 regarding the interaction between methanol and zeolite.

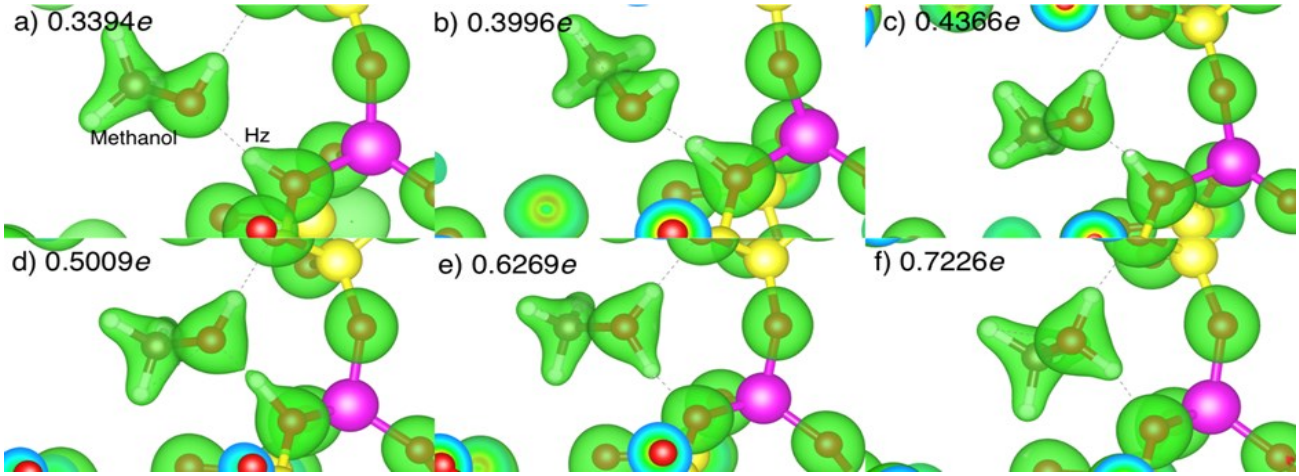

Figure 5. The electron density of methanol in selected structural configurations showing the interaction between methanol and Hz. An isosurface of 0.15 au is applied for all figures. The net molecular charge is given for methanol including the Hz charge. Al, Si, O, C and H are shown as magenta, yellow, red, brown and white colour, respectively.

Table 1. List of several studies on the use of zeolite for methanol transformation.

No	Type of zeolite	Methods or setup	Reference
1	H-ZSM-5	Catalytic reactor at 130 °C and 190 °C	[39]
2	H-zeolite	Calculation with MP2 method and microkinetic studies	[40]
3	H-ZSM-5	AIMD at 670 K and DFT calculation	[41]
4	H-MOR	Catalytic reactor at 100 °C to 300 °C	[42]
5	H-ZSM-5	AIMD at 300 K	[15]
6	HSAPO-34	DFT	[43]
7	H-ZSM-5 and H-SAPO-34	Characterization using multinuclear solid-state NMR	[44]
8	H-ZSM-5	Catalytic reactor at 100 – 350 °C	[45]
9	H-Mordenite	Catalytic reactor at 473 K to 573 K	[46]

The presence of methoxonium ion is confirmed by the net molecular charge of $[CH_3OH_2]^+$ to give +0.72*e* based on the Mulliken partition (see Figure 5), while the zeolite has negatively charge of −0.72*e* due to the interaction of proton with methanol. Consequently, the bond distance of oxygen of methanol (Om) and carbon of methanol (Cm) is also slightly elongated. At 300 K, the Om−Cm has bond distance of 1.37 Å at the lowest and 1.59 Å at the longest distance, while the longest Om−Cm at 573K is at 1.62 Å (see Figure 4(e)). As a reference, the Om-Cm bond distance of an isolated methanol is 1.43 Å. Therefore, the interaction between H (Brönsted acid sites) and Om lead to the possible activation of methanol which is beneficial for transforming methanol to other valuable compounds, such as olefins and hydrocarbon.

To further confirm the interaction between methanol and zeolite surface, the electron density of selected configurations along the production phase was assessed as given in Figure 5. When the distance between methanol dan Hz is slightly longer at 1.62 Å (Figure 5(a)), the electron density shows a gap between those components indicating no interaction. This is further confirmed by calculating the net molecular charge of methanol plus Hz to give 0.3394e. When the net charge of Hz is not included, the net charge of methanol will be 0.1042e which is close to be a neutral molecule of methanol. The distance between methanol and Hz is becoming shorter inducing a distortion in the electronic density while increasing the net molecular charge of methanol plus Hz (see Figure 5(b)-(d)). Further decrease in distance, Hz is attached fully to methanol to give

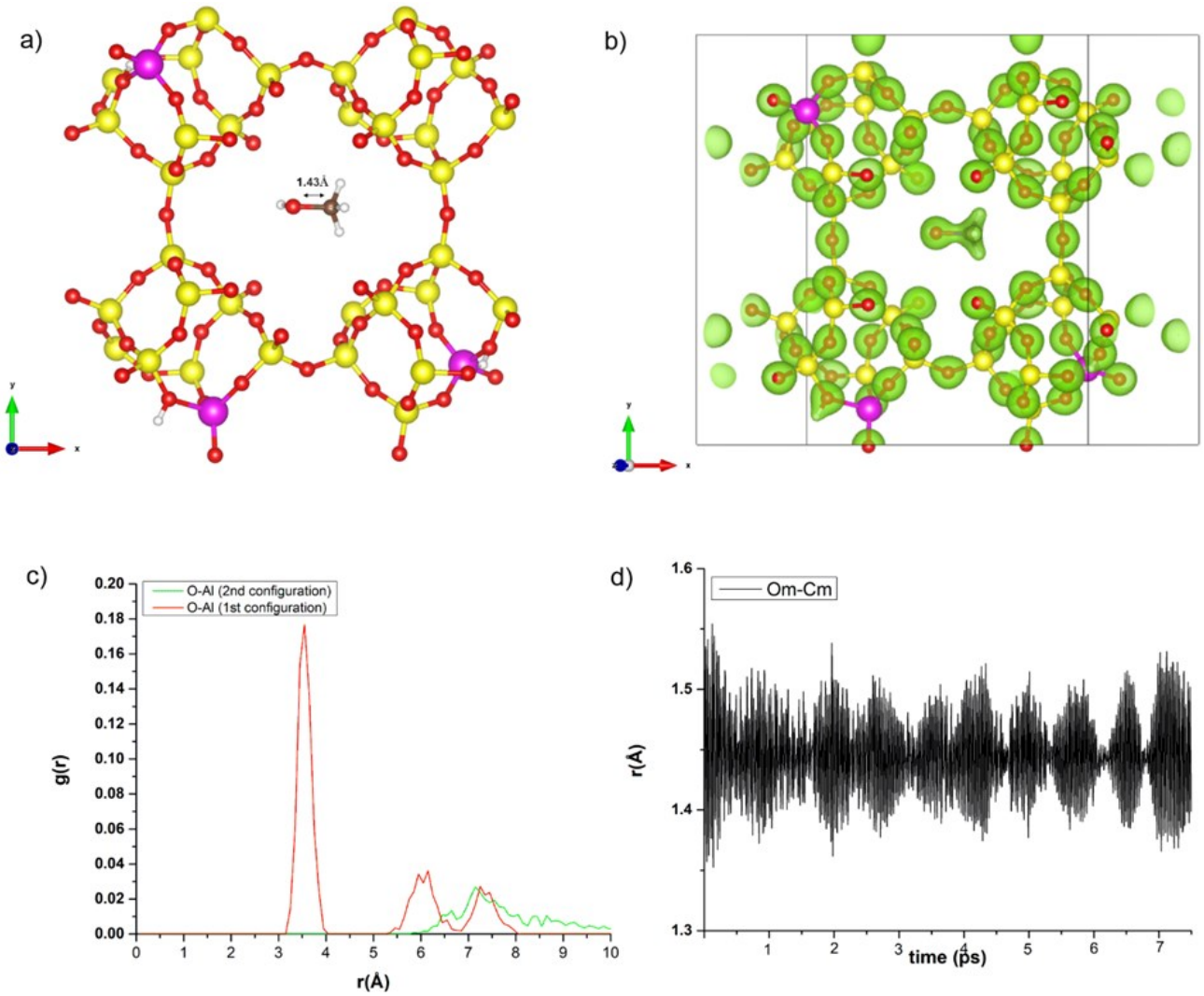

Figure 6. The optimized structure (a) and electron density (b) of the HEU zeolite in the presence of methanol obtained from the static DFT. The RDF of oxygen of methanol to Al (a) and the bond distance of Om to Cm along the production phase of AIMD (b) are also given.

$[CH_3OH_2]^+$ ion with the net molecular charge of 0.7226*e* as seen in Figure 5(e) and (f).

3.3 Effect of Brönsted Acid Location

The design of zeolite catalyst might require adjusting the number or location of proton acting as the Brönsted acid sites. This can be performed by varying the Si/Al ratio and structural investigation to locate their position within the zeolite framework [47–49]. In this study, methanol was placed inside the largest pore (10MR) where the proton location is not facing out that pore. In Figure 6(a), the optimized structure of Heulandite structure in the presence of methanol is given indicating different behaviour of methanol which is relatively longer in distance to the surface of the 10MR ring. Since minimum interaction might occur, the bond length of oxygen of methanol (Om) to the carbon of methanol (Cm) is shorter than it in the first configuration (see Figure 3(a)) with a value of 1.43 Å. The electron density of Heulandite structure in the presence of methanol also indicates less interaction as no possible electron density overlap as seen in Figure 6(b). In addition, the adsorption energy is at −42.1 kJ/mol which is higher than the first configuration. This energy consideration indicates that methanol is preferably interacting with the bulk zeolite through possible Brönsted acid sites.

Further investigation is conducted by using AIMD approach. The spatial location of oxygen of methanol (Om) to aluminium can be differentiate according to the RDF as given in Figure 6(c). When proton is also located on the surface of the 10MR pore, methanol (Om) is relatively close to the Al atom with an approximate distance of ~3.5 Å indicating interaction between methanol and proton as shown by the red line of Figure 6(c). In the second configuration where proton is not facing out the 10MR pore, the RDF of Om to Al has the closest distance at approximately ~5.5 Å (see the blue line of Figure 6(c)). This condition might lead to the less activation of methanol to become more reactive species. The less activation of methanol can also be seen from the bond distance of Om−Cm with the lowest distance at 1.35 Å and the longest distance is at 1.55 Å as given in Figure 6(d).

4. Conclusion

The interaction between methanol and Heulandite type zeolite has been assessed to give an atomic insight how methanol can be activated into possible cationic species of $[CH_3OH_2]^+$ in the presence of acid sites on the zeolite surface. The interaction can be identified based on the structural behavior of methanol and the acid sites. An elongated Oz−Hz bond is observed indicating the transfer of proton from the zeolite surface towards methanol (Om). This species can be confirmed from the electronic density plot. When methanol is still far from proton, electron density shows no overlap, however when methanol has interacted with proton, an overlap of electronic density can be observed. In addition, the effect of proton location also influences the formation of this cationic species. When the location of proton is not accessible to methanol, a longer possible distance between Om and Al in the zeolite framework is observed as indicated by the RDF of Om−Al. This study provides an insight into the use of Heulandite type zeolite as catalyst for methanol transformation.

Acknowledgement

This research was supported by the Department of Chemistry, the Faculty of Mathematics and Natural Sciences, Universitas Gadjah Mada that is greatly appreciated**.**

References

[1] Davis, M.E. (2014). Zeolites from a materials chemistry perspective. *Chemistry of Materials*, 26(1), 239–245. DOI: 10.1021/cm401914u.

[2] Larsen, S.C. (2007). Nanocrystalline zeolites and zeolite structures: Synthesis, characterization, and applications. *Journal of Physical Chemistry C*, 111(50), 18464–18474. DOI: 10.1021/JP074980M.

[3] Database of Zeolite Structures. http://www.iza-structure.org/databases/. Accessed 4 Apr 2022.

[4] Król, M. (2020). Natural vs. Synthetic zeolites. *Crystals*, 10(7), 1–8. DOI: 10.3390/cryst10070622.

[5] Liang, Y., Jacobson, A.J., Rimer, J.D. (2021). Strontium Ions Function as Both an Accelerant and Structure-Directing Agent of Chabazite Crystallization. *ACS Materials Letters*, 3(2), 187–192. DOI: 10.1021/acsmaterialslett.0C00460.

[6] Lee, H., Shin, J., Hong, S.B. (2021). Tetraethylammonium-Mediated Zeolite Synthesis via a Multiple Inorganic Cation Approach. *ACS Materials Letters*, 3(4), 308–312. DOI: 10.1021/acsmaterialslett.1C00034.

[7] Blay, V., Louis, B., Miravalles, R., Yokoi, T., Peccatiello, K.A., Clough, M., Yilmaz, B. (2017). Engineering zeolites for catalytic cracking to light olefins. *ACS Catalysis*, 7(10), 6542–6566. DOI: 10.1021/acscatal.7B02011.

[8] Shirono, K., Endo, A., Daiguji, H. (2005). Molecular dynamics study of hydrated faujasite-type zeolites. *Journal of Physical Chemistry B*, 109(8), 3446–3453. DOI: 10.1021/JP047293T.

[9] Ahunbay, M.G. (2011). Monte carlo simulation of water adsorption in hydrophobic MFI zeolites with hydrophilic sites. *Langmuir*, 27(8), 4986–4993. DOI: 10.1021/LA200685C.

[10] Zhou, T., Bai, P., Siepmann, J.I., Clark, A.E. (2017). Deconstructing the Confinement Effect upon the Organization and Dynamics of Water in Hydrophobic Nanoporous Materials: Lessons Learned from Zeolites. *Journal of Physical Chemistry C*, 121(40), 22015–22024. DOI: 10.1021/acs.jpcc.7B04991.

[11] Wu, J.Y., Liu, Q.L., Xiong, Y., Zhu, A.M., Chen, Y. (2009). Molecular simulation of water/alcohol mixtures' adsorption and diffusion in zeolite 4a membranes. *Journal of Physical Chemistry B*, 113(13), 4267–4274. DOI: 10.1021/JP805923K.

[12] Stepanov, A.G., Alkaev, M.M., Shubin, A.A. (2000). Molecular dynamics of iso-butyl alcohol inside zeolite H-ZSM-5 as studied by deuterium solid-state NMR spectroscopy. *Journal of Physical Chemistry B*, 104(32), 7677–7685. DOI: 10.1021/JP000581E.

[13] Pambudi, F.I., Prasetyo, N. (2021). Insight into the structure of the heulandite-type zeolite containing aromatic compounds using periodic density functional theory. *Materials Today Communications*, 26, 102028. DOI: 10.1016/j.mtcomm.2021.102028.

[14] Nastase, S.A.F., Logsdail, A.J., Richard, C., Catlow, A. (2021). QM/MM study of the reactivity of zeolite bound methoxy and carbene groups. *Phys Chem Chem Phys*, 23, 17634. DOI: 10.1039/d1cp02535j.

[15] Nastase, S.A.F., Cnudde, P., Vanduyfhuys, L., De Wispelaere, K., Speybroeck, V. Van, Richard, C., Catlow, A., Logsdail, A.J. (2020). Mechanistic Insight into the Framework Methylation of H-ZSM-5 for Varying Methanol Loadings and Si/Al Ratios Using First-Principles Molecular Dynamics Simulations. https://doi.org/10.1021/acscatal.0c01454

[16] Tian, P., Wei, Y., Ye, M., Liu, Z. (2015). Methanol to olefins (MTO): From fundamentals to commercialization. *ACS Catalysis*, 5(3), 1922–1938. DOI: 10.1021/acscatal.5B00007.

[17] Stöcker, M. (1999). Methanol-to-hydrocarbons: catalytic materials and their behavior. *Microporous and Mesoporous Materials*, 29(1–2), 3–48. DOI: 10.1016/S1387-1811(98)00319-9.

[18] Mahyuddin, M.H., Staykov, A., Shiota, Y., Miyanishi, M., Yoshizawa, K. (2017). Roles of Zeolite Confinement and Cu-O-Cu Angle on the Direct Conversion of Methane to Methanol by [Cu2(μ-O)]2+-Exchanged AEI, CHA, AFX, and MFI Zeolites. *ACS Catalysis*, 7(6), 3741–3751. DOI: 10.1021/acscatal.7B00588.

[19] Chen, J., Li, J., Wei, Y., Yuan, C., Li, B., Xu, S., Zhou, Y., Wang, J., Zhang, M., Liu, Z. (2014). Spatial confinement effects of cage-type SAPO molecular sieves on product distribution and coke formation in methanol-to-olefin reaction. *Catalysis Communications*, 46, 36–40. DOI: 10.1016/j.catcom.2013.11.016.

[20] Li, J., Wei, Y., Chen, J., Xu, S., Tian, P., Yang, X., Li, B., Wang, J., Liu, Z. (2015). Cavity controls the selectivity: Insights of confinement effects on MTO reaction. *ACS Catalysis*, 5(2), 661–665. DOI: 10.1021/CS501669K.

[21] Gao, P., Xu, J., Qi, G., Wang, C., Wang, Q., Zhao, Y., Zhang, Y., Feng, N., Zhao, X., Li, J., Deng, F. (2018). A Mechanistic Study of Methanol-to-Aromatics Reaction over Ga-Modified ZSM-5 Zeolites: Understanding the Dehydrogenation Process. *ACS Catalysis*, 8(10), 9809–9820. DOI: 10.1021/acscatal.8B03076.

[22] Qian, K., Li, L., Chen, P., Xiu, Y., E, Y., Gies, H. (2021). Copper-nickel doped LTA zeolite as a high- efficiency methanol oxidation reaction catalyst in alkaline solution. *International Journal of Hydrogen Energy*, 46(46), 23898–23905. DOI: 10.1016/j.ijhydene.2021.04.155.

[23] Li, X., Sun, Q., Li, Y., Wang, N., Lu, J., Yu, J. (2014). Confinement effect of zeolite cavities on methanol-to-olefin conversion: A density functional theory study. *Journal of Physical Chemistry C*, 118(43), 24935–24940. DOI: 10.1021/JP505696M.

[24] Zhao, D., Cleare, K., Oliver, C., Ingram, C., Cook, D., Szostak, R., Kevan, L. (1998). Characteristics of the synthetic heulandite-clinoptilolite family of zeolites. *Microporous and Mesoporous Materials*, 21(4–6), 371–379. DOI: 10.1016/S1387-1811(98)00131-0.

[25] Schmidt, J.E., Xie, D., Davis, M.E. (2015). High-silica, heulandite-type zeolites prepared by direct synthesis and topotactic condensation. *Journal of Materials Chemistry A*, 3(24), 12890–12897. DOI: 10.1039/c5ta02354h.

[26] Laboy, M.M., Santiago, I., López, G.E. (1999). Computing Adsorption Isotherms for Benzene, Toluene, and p-Xylene in Heulandite Zeolite. *Industrial and Engineering Chemistry Research*, 38(12), 4938–4945. DOI: 10.1021/ie980732o.

[27] Hernández, M.A., Corona, L., Gonzalez, A.I., Rojas, F., Lara, V.H., Silva, F. (2005). Quantitative Study of the Adsorption of Aromatic Hydrocarbons (Benzene, Toluene, and p-Xylene) on Dealuminated Clinoptilolites. *Industrial and Engineering Chemistry Research*, 44(9), 2908–2916. DOI: 10.1021/IE049276W.

[28] Channon, Y.M., Catlow, C.R.A., Gorman, A.M., Jackson, R.A. (1998). Grand Canonical Monte Carlo Investigation of Water Adsorption in Heulandite-type Zeolites. *Journal of Physical Chemistry B*, 102(21), 4045–4048. DOI: 10.1021/JP980483H.

[29] Ockwig, N.W., Cygan, R.T., Hartl, M.A., Daemen, L.L., Nenoff, T.M. (2008). Incoherent Inelastic Neutron Scattering Studies of Nanoconfined Water in Clinoptilolite and Heulandite Zeolites. *Journal of Physical Chemistry C*, 112(35), 13629–13634. DOI: 10.1021/JP803770V.

[30] Baek, W., Ha, S., Hong, S., Kim, S., Kim, Y. (2018). Cation exchange of cesium and cation selectivity of natural zeolites: Chabazite, stilbite, and heulandite. *Microporous and Mesoporous Materials*, 264, 159–166. DOI: 10.1016/j.micromeso.2018.01.025.

[31] Sánchez-Velandia, J.E., Gelves, J.F., Márquez, M.A., Dorkis, L., Villa, A.L. (2020). Catalytic Isomerization of α-Pinene Epoxide Over a Natural Zeolite. *Catalysis Letters*, 150(11), 3132–3148. DOI:10.1007/s10562-020-03225-9.

[32] Kühne, T.D., Iannuzzi, M., Del Ben, M., Rybkin, V. V., Seewald, P., Stein, F., Laino, T., Khaliullin, R.Z., Schütt, O., Schiffmann, F., Golze, D., Wilhelm, J., Chulkov, S., Bani-Hashemian, M.H., Weber, V., Borštnik, U., Taillefumier, M., Jakobovits, A.S., Lazzaro, A., Pabst, H., Müller, T., Schade, R., Guidon, M., Andermatt, S., Holmberg, N., Schenter, G.K., Hehn, A., Bussy, A., Belleflamme, F., Tabacchi, G., Glöß, A., Lass, M., Bethune, I., Mundy, C.J., Plessl, C., Watkins, M., VandeVondele, J., Krack, M., Hutter, J. (2020). CP2K: An electronic structure and molecular dynamics software package - Quickstep: Efficient and accurate electronic structure calculations. *The Journal of Chemical Physics*, 152(19), 194103. DOI: 10.1063/5.0007045.

[33] Cruciani, G. (2006). Zeolites upon heating: Factors governing their thermal stability and structural changes. *Journal of Physics and Chemistry of Solids*, 67(9–10), 1973–1994. DOI: 10.1016/j.jpcs.2006.05.057.

[34] Alberti, A. (1973). The structure type of heulandite B (heat-collapsed phase). *TMPM Tschermaks Mineralogische und Petrographische Mitteilungen*, 19(3), 173–184. DOI: 10.1007/BF01167426.

[35] Khobaer, T.M., Kuribayashi, T., Komatsu, K., Kudoh, Y. (2008). The partially dehydrated structure of natural heulandite: An in situ high temperature single crystal X-ray diffraction study. *Journal of Mineralogical and Petrological Sciences*, 103(2), 61–76. DOI: 10.2465/jmps.070306.

[36] Valdiviés Cruz, K., Lam, A., Zicovich-Wilson, C.M. (2014). Periodic quantum chemical studies on anhydrous and hydrated acid clinoptilolite. *Journal of Physical Chemistry A*, 118(31), 5779–5789. DOI: 10.1021/jp410754a.

[37] Uzunova, E.L., Mikosch, H. (2013). Cation site preference in zeolite clinoptilolite: A density functional study. *Microporous and Mesoporous Materials*, 177, 113–119. DOI: 10.1016/j.micromeso.2013.05.003.

[38] Koyama, K., Takeuchi, Y. (2014). Clinoptilolite: the distribution of potassium atoms and its role in thermal stability. *Zeitschrift für Kristallographie - Crystalline Materials*, 145(1–6), 216–239. DOI: 10.1524/zkri.1977.145.16.216.

[39] Trypolskyi, A., Zhokh, A., Gritsenko, V., Chen, M., Tang, J., Strizhak, P. (2021). A kinetic study on the methanol conversion to dimethyl ether over H-ZSM-5 zeolite. *Chemical Papers*, 75(7), 3429–3442. DOI: 10.1007/S11696-021-01586-Y.

[40] Park, J., Cho, J., Park, M.J., Lee, W.B. (2021). Microkinetic modeling of DME synthesis from methanol over H-zeolite catalyst: Associative vs. dissociative pathways. *Catalysis Today*, 375, 314–323. DOI: 10.1016/J.CATTOD.2020.02.011.

[41] Moors, S.L.C., De Wispelaere, K., Van Der Mynsbrugge, J., Waroquier, M., Van Speybroeck, V. (2013). Molecular dynamics kinetic study on the zeolite-catalyzed benzene methylation in ZSM-5. *ACS Catalysis*, 3(11), 2556–2567. DOI: 10.1021/CS400706E.

[42] Aboul-Fotouh, S.M.K., Aboul-Gheit, N.A.K., Hassan, M.M.I. (2011). Conversion of Methanol Using Modified H-MOR Zeolite Catalysts. *Chinese Journal of Catalysis*, 32(3–4), 412–417. DOI: 10.1016/S1872-2067(10)60187-8.

[43] Wang, Z., Chen, X.F. (2021). A periodic density functional theory study on methanol adsorption in HSAPO-34 zeolites. *Chemical Physics Letters*, 771, 138532. DOI: 10.1016/j.cplett.2021.138532.

[44] Salehirad, F., Anderson, M.W. (1998). Solid-state NMR studies of adsorption complexes and surface methoxy groups on methanol-sorbed microporous materials. *Journal of Catalysis*, 177(2), 189–207. DOI: 10.1006/jcat.1998.2096.

[45] Aboul-Fotouh, S.M.K., Ali, L.I., Naghmash, M.A., Aboul-Gheit, N.A.K. (2017). Effect of the Si/Al ratio of HZSM-5 zeolite on the production of dimethyl ether before and after ultrasonication. *Journal of Fuel Chemistry and Technology*, 45(5), 581–588. DOI: 10.1016/S1872-5813(17)30030-0.

[46] Bandiera, J., Naccache, C. (1991). Kinetics of methanol dehydration on dealuminated H-mordenite: Model with acid and basic active centres. *Applied Catalysis*, 69(1), 139–148. DOI: 10.1016/S0166-9834(00)83297-2.

[47] Huo, H., Peng, L., Gan, Z., Grey, C.P. (2012). Solid-state MAS NMR studies of Brønsted acid sites in zeolite H-Mordenite. *Journal of the American Chemical Society*, 134(23), 9708–9720. DOI: 10.1021/JA301963E.

[48] Lukyanov, D.B., Vazhnova, T., Cherkasov, N., Casci, J.L., Birtill, J.J. (2014). Insights into Brønsted acid sites in the zeolite mordenite. *Journal of Physical Chemistry C*, 118(41), 23918–23929. DOI: 10.1021/JP5086334.

[49] Peng, L., Chupas, P.J., Grey, C.P. (2004). Measuring Brønsted acid densites in zeolite HY with diphosphine molecules and solid state NMR spectroscopy. *Journal of the American Chemical Society*, 126(39), 12254–12255. DOI: 10.1021/JA0467519.